Title

Dual Stromal Targeting Sensitizes Pancreatic Adenocarcinoma for Anti-Programmed Cell Death Protein 1 Therapy.

Journal

Gastroenterology, 163(5)

Authors

Blair, Alex
Wang, Jianxin
Davelaar, John
et al.

Publication Date

2022-11-01

DOI

10.1053/j.gastro.2022.06.027

Peer reviewed

HHS Public Access

Author manuscript

Gastroenterology. Author manuscript; available in PMC 2023 November 01.

Published in final edited form as:

Gastroenterology. 2022 November ; 163(5): 1267–1280.e7. doi:10.1053/j.gastro.2022.06.027.

Dual stromal targeting sensitizes pancreatic adenocarcinoma for anti-PD-1 therapy:

Dual stromal targeting in Pancreatic Cancer

Alex B. Blair[1,2,3,4,5], **Jianxin Wang**[1,4,5], **John Davelaar**[8], **Andrew Baker**[1], **Keyu Li**[1,4,5], **Nan Niu**[1,4,5], **Junke Wang**[1,4,5], **Yingkuan Shao**[1,4,5], **Vanessa Funes**[1,3,4,5], **Pan Li**[1,4,5], **Jonathan A. Pachter**[6], **Dan Maneval**[6], **Felipe Dezem**[8], **Jasmine Plummer**[8], **Keith Syson Chan**[8], **Jun Gong**[8], **Andrew E. Hendifar**[8], **Stephen J. Pandol**[8], **Richard Burkhart**[1,2,3], **Yuqing Zhang**[7], **Lei Zheng**[1,2,3,4,5], **Arsen Osipov**[1,3,4,5,8]

[1]Department of Oncology and the Sidney Kimmel Comprehensive Cancer Center, Johns Hopkins University School of Medicine, Baltimore, MD

[2]Department of Surgery, Johns Hopkins University School of Medicine, Baltimore, MD

[3]The Multidisciplinary Gastrointestinal Cancer Laboratories Program, the Sidney Kimmel Comprehensive Cancer Center, Johns Hopkins University School of Medicine, Baltimore, MD

[4]The Bloomberg-Kimmel Institute for Cancer Immunotherapy, Johns Hopkins University School of Medicine, Baltimore, MD

[5]The Pancreatic Cancer Precision Medicine Center of Excellence Program, Johns Hopkins University School of Medicine, Baltimore, MD

[6]Verastem Oncology, Needham, MA

[7]Department of Medicine, the University of Oklahoma Health Sciences Center, Oklahoma City

[8]Cedars-Sinai Medical Center, Los Angeles, CA

Abstract

Corresponding authors: Lei Zheng, M.D., Ph.D. lzheng6@jhmi.edu , 1650 Orleans Street, CRB1 Room 351, Baltimore, MD 21231; Tel: 410-502-6241; Fax: 410-614-8216.; **Arsen Osipov, M.D.** arsen.osipov@cshs.org, 8700 Beverly Blvd., North Tower, Lower Level. AC1044, Los Angeles, CA, 90048; Tel: 310-423-6313: Fax 424-314-8777.

Authors' contributions

AB, JW, LZ, AO developed methodology. AB, JW, NN, AO, AB(Baker), VF, JD, KL, PL, YS, JP, DM, LZ, AO acquired data. AB, JW, AO, AB(Baker), FD JD, KC, YZ, JG, AH, SP, JP(Plummer), VF, RB, YS, LZ analyzed and interpreted data. Verastem provided critical materials. AB, KC, YZ, SP, LZ, AO wrote, reviewed, and/or revised the manuscript. LZ, JP, DM, AB, AO developed the concept and design the study. AO, LZ supervised the study.

Disclosures:

LZ receives grant support from Bristol-Meyer Squibb, Merck, AstraZeneca, iTeos, Amgen, NovaRock, Inxmed, and Halozyme. LZ is a paid consultant/Advisory Board Member at Biosion, Alphamab, NovaRock, Xilio, QED, Natera, Novagenesis, Ambrx, Snow Lake Capitals, Amberstone, and Mingruizhiyao. LZ holds shares at Alphamab and Mingruizhiyao. JP is employed by Verastem Oncology. DM is employed by Halozyme. All other authors declare no competing interests.

Background and Aims: The stroma in pancreatic ductal adenocarcinoma (PDAC) contributes to its immunosuppressive nature and therapeutic resistance. Herein we sought to modify signaling and enhance immunotherapy efficacy by targeting multiple stromal components through both intracellular and extracellular mechanisms.

Methods: A murine liver metastasis syngeneic model of PDAC was treated with focal adhesion kinase inhibitor (FAKi), anti-PD-1 antibody and stromal hyaluronan (HA) degradation by PEGPH20 to assess immune and stromal modulating effects of these agents and their combinations.

Results: The results showed that HA degradation by PEGPH20 and reduction in phosphorylated FAK expression by FAKi leads to improved survival in PDAC-bearing mice treated with anti-PD-1 antibody. HA degradation in combination with FAKi and anti-PD-1 antibody increases T-cell infiltration and alters T-cell phenotype towards effector memory T-cells. FAKi alters the expression of T-cell modulating cytokines and leads to changes in T-cell metabolism and increases in effector T-cell signatures. HA degradation in combination with anti-PD-1 antibody and FAKi treatments reduces granulocytes including granulocytic-MDSCs and decreases CXCR4 expressing myeloid cells, particularly the CXCR4 expressing granulocytes. Anti-CXCR4 antibody combined with FAKi and anti-PD-1 antibody significantly decreases metastatic rates in the PDAC liver metastasis model.

Conclusion: This represents the first preclinical study to identify synergistic effects of targeting both intracellular and extracellular components within the PDAC stroma and supports testing anti-CXCR4 antibody in combination with FAKi as a PDAC treatment strategy.

LAY SUMMARY

Simultaneous targeting of both intracellular and extracellular components of the stroma in pancreatic cancer, can alter the tumor microenvironment, thereby improving immunotherapy response.

Keywords

Pancreatic ductal adenocarcinoma; FAK; anti-PD-1 antibody; hyaluronan; CXCR4

Pancreatic ductal adenocarcinoma (PDAC) continues to have dismal rates of overall survival due to its treatment refractory nature to most standard therapies[1]. The development of immunotherapy has revolutionized the treatment paradigm for numerous malignancies[2]. However, in PDAC, checkpoint inhibition has been met with failure in large part due to its immunosuppressive tumor microenvironment (TME). PDAC produces an intense desmoplastic reaction, including a well-defined stroma and significant hyaluronic acid (HA) deposition[3, 4]. HA is an extracellular glycosaminoglycan constituent of tissues that binds to proteoglycans forming the dense extracellular matrix (ECM). This stroma also contributes to a complex immunosuppressive signaling axis to regulate cancer growth, manipulate immune surveillance, and limit the efficacy of systemic therapies[5-9].

Agents targeting components of the PDAC stroma have been investigated in preclinical and phase I-III studies with mixed results[9-12]. PEGPH20 is a PEGylated recombinant human

hyaluronidase which degrades stromal HA following systemic administration. Preclinical studies in murine PDAC models with PEGPH20 and chemotherapy have been shown to decrease intratumoral HA and increase drug delivery, resulting in significantly prolonged survival[13-15]. However, clinical studies, culminating with the phase III HALO 301, did not meet primary endpoints and clinical development of PEGPH20 was halted[16]. Though these results suggest that direct HA depletion via PEGPH20 may not be enough to overcome the chemotherapeutic resistance of PDAC, PEGPH20 provides a platform through which to further study the immunosuppressive TME and its stromal interplay within PDAC. In our recently published study, we found that stromal depletion of HA with PEGPH20 combined with a GM-CSF secreting allogeneic tumor cell vaccine (GVAX) decreases immunosuppressive signaling axis expression, enhances $CD8^+$ T-cell infiltration, effector activity and improves survival compared to single agent therapies in mice[9].

While HA is a major component of extracellular stroma, focal adhesion kinases (FAK) appear to regulate intracellular signaling in stromal and myeloid cells[17]. FAK has been implicated in increased pathologic fibrosis, cytokine release, and inflammation. Inhibition of the FAK pathway in neoplastic cells has been shown to modulate pancreatic stellate cells leading to a decrease in immunosuppressive cells including myeloid-derived suppressor cells (MDSCs), tumor associated macrophages (TAMs), and regulatory T-cells (Treg) in PDAC mouse models, accompanied by increased $CD8^+$ T-cells and decreased collagen deposition[11]. Defactinib is a clinical ATP-competitive inhibitor of both FAK and proline rich tyrosine kinase 2 (pyk2) currently investigated in clinical trials for PDAC (NCT03727880). The dual inhibition role of defactinib is important, as Pyk2 upregulation has been identified as a critical mechanism of feedback following FAK inhibition[18].

Previously, we discovered that targeting the stroma by degrading HA with PEGPH20 in combination with GVAX decreases expression of CXCL12 in fibroblasts and CXCR4 in myeloid cells corresponding to increased effector memory $CD8^+$ T-cells (Tem) infiltration[9]. We hypothesized that targeting FAK and anti-PD-1 antibody may increase T-cell infiltration as an alternative to GVAX and synergize with extracellular modulation by PEGPH20 to decrease immunosuppressive myeloid cells. Additionally, previous studies have investigated the role of FAK inhibitor (FAKi) in the tumor, whereas the effects of FAKi in the TME remains unknown[11, 19].

Thus, in this investigation we utilized PEGPH20 as a platform to target extracellular signaling within the PDAC TME, and examine the effect of dual stromal targeting in sensitizing PDAC for anti-PD-1 therapy: one with FAKi and the second with CXCR4 inhibition through HA degradation by PEGPH20. More recently, the combination of anti-PD-1 antibody and CXCR4 inhibitor showed durable antitumor responses, albeit with low objective response rates, in treating metastatic PDAC patients[20]. Therefore, we also examined whether directly targeting CXCR4 enhances the antitumor activity of anti-PD-1 antibody in combination with FAK inhibition in the preclinical model of PDAC.

Methods

Cell lines

The KPC tumor cell line is a previously established PDAC cell line derived from a genetically engineered mouse model, the KPC model (LSL-Kras(G12D/+);LSL-Trp53(R172H/+);Pdx-1-Cre), backcrossed to the C57Bl/6 background and cultured as previously described[21, 22].

Mouse models and in vivo treatments

Wild-type C57Bl/6 female mice (6–8 weeks, Harlan Laboratories) were maintained in accordance with the Institutional Animal Care and Use Committee (IACUC) guidelines. Mice considered to have reached a "survival endpoint", including hunched posture, lethargy, dehydration, and rough coat, were humanely euthanized. The IACUC mouse protocol and "survival endpoint" identification was maintained by third-party management. As previously described, the hemispleen tumor inoculation technique was performed on Day 0; and untreated mice die of diffuse liver metastases in approximately 30-60 days[23,24]. For the orthotopic model, 2×10^6 KPC cells were subcutaneously injected into the flanks of female C57Bl/6 mice. After 1 to 2 weeks, subcutaneous tumors were harvested, divided into 2 mm^3 pieces, and implanted into the distal portion of the pancreas of new syngeneic female C57BI/6 mice. Previously, we demonstrated similar CAF and HA expression between the orthotopic model and the hemispleen model[9]. The orthotopic model was chosen for isolating $CD8^+$ T-cells and CAFs to compare with RNA sequencing results from previous studies.

PEGPH20 (40μg/kg, provided by Halozyme Therapeutics, Inc.) was administered intravenously by tail vein injection semiweekly (BIW) starting on post-operative day (POD) 6 when numerous micrometastases with HA-expressing stroma have formed, as shown previously[9]. Because defactinib has relatively poor pharmacokinetics in mice, its mouse surrogate, VS-4718, employed in murine experimental models, was utilized. Defactinib and VS-4718 have similar potencies to inhibit FAK in vitro. FAKi, VS-4718 (50mg/kg, provided by Verastem Oncology), was administered by oral gavage twice-daily (BID) beginning on POD6. Anti-PD-1 antibody (5mg/kg; RMP1-14, BioXcell) or control IgG (5mg/kg; 2A3 IgG2a, BioXcell) were administered by intraperitoneal injection BIW starting on POD7. Anti-CXCR4 antibody (10mg/kg, mCXCR4.8-mG1, provided by BMS) or control (IgG1, MOPC-21, BioXcell) was administered by intraperitoneal injection BIW starting on POD7. Mice were monitored daily for survival analysis and euthanized by CO_2 inhalation if IACUC-approved criteria were met, or at experiment conclusion (Figure 1A).

Tumor processing and tumor-infiltrating leukocyte isolation

Mouse livers with diffuse metastases were collected on POD16 following the hemispleen procedure for analysis of fibroblasts and tumor-infiltrating leukocytes (TIL). Each was processed sequentially through 40-μm and 100-μm nylon filters and suspended in 20 mL of CTL medium. Suspensions were centrifuged at 1,500 rpm for 5 minutes. Cell pellets were suspended in 4 mL of ACK lysis (Quality Biological) and centrifuged at 1,500 rpm for 5 minutes. Cell pellets were resuspended in 6 mL 80% Percoll (GE Healthcare LifeSciences),

overlaid with 6 mL 40% Percoll, and centrifuged at room temperature for 25 minutes at 3,200 rpm. The immune cell layer was removed and quenched with 30 mL of CTL media.

Flow cytometry

TILs were stained with Live/Dead Aqua Dead Cell Kit (Invitrogen) for 30 minutes on ice, washed with PBS, and then blocked with rat anti-mouse Fc antibody (CD16/CD32 clone 2.4G2, BD Biosciences) in FACS buffer for 10 minutes. After blocking, cells were stained with fluorophore-conjugated antibodies (Supplemental Table S1) for 1 hour on ice. Cells were washed, resuspended in FACS buffer (Hanks Balanced Salt solution (Sigma), 2% bovine calf serum (Sigma), 0.1% sodium azide (Sigma) 0.1% HEPES), and assayed on a Cytoflex flow cytometer (Beckman Coulter). Live Dead Aqua and the plot of side scatter versus forward scatter identified initial gated live immune cell counts. The “total number” of immune cells infiltrating an analyzed tumor specimen was determined by the gated count by FACS analysis normalized to the total isolated TIL of each mouse. The “percentage” of immune cells represents the proportion of a specific immune cell subtype gated among the live immune cell counts or other cell subtypes.

Immunohistochemistry

Following the hemispleen procedure, mice were sacrificed on POD16 and livers were fixed in formalin for investigation of HA and phosphorylated FAK (pFAK) expression. Slides were sectioned from the formalin-fixed paraffin-embedded (FFPE) blocks and stained for HA as described previously[25]. Slides were stained for pFAK using the following sequence: anti-phospho-FAK rabbit monoclonal antibody (31H5L17, ThermoFisher, 1:1000) for 90 minutes, biotinylated goat anti-rabbit IgG antibody (BA-1000, Vector Labs, 1:200) for 30 minutes, avidin-biotin-peroxidase complex (PK-4000, Vector Labs) for 30 minutes, and developed using DAB hydrochloride (SK-4100, Vector Labs). Slides were scanned and analyzed using HALO Image Analysis Software (Indica Labs).

RNA sequencing

Dissected orthotopic KPC tumors were digested into single cells and pooled from the same group. Fibroblasts were individually obtained within this single cell suspension via a fibroblast activation protein^{+} (FAP) specific direct isolation technique as described previously[9]. The Cellection Biotin Binder Kit (Life Technologies) was used to conjugate beads with sheep anti-human FAP biotinylated affinity-purified antibody (R&D Systems Inc.). The human FAP gene is conserved with high homology to mouse FAP (HomoloGene)[26]. These FAP^{+} beads were then incubated with the cell suspension and extracted via magnetic cell separation. CD8^{+} cells were isolated from TILs using CD8^{+} isolation kits (Life Technologies). TRIzol Reagent (Thermo Fisher Scientific) was used to extract RNA from isolated CAFs and CD8^{+} T-cells and whole transcriptomic RNA sequencing was performed at BGI Americas.

Statistical analysis

Statistical analyses and graphing were performed using GraphPad Prism software. Kaplan–Meier curves and log-rank tests were performed for survival estimates. One-way ANOVA

or Student's t-tests were applied to compare the mean value among or between groups. A p-value<0.05 was considered statistically significant.

Study approval

De-identified human PDAC resection specimens were obtained from the clinical trial (NCT02451982) patients who underwent surgery at the Johns Hopkins Hospital under the Johns Hopkins Medical Institution Institutional Review Board (IRB) approved protocol (IRB00050517).

RESULTS

PEGPH20 targets the stroma of liver metastases of PDAC and enhances survival of PDAC-bearing mice treated by FAKi in combination with anti-PD-1 antibody

To assess whether PEGPH20 can synergize with FAKi to potentiate the antitumor immune response of anti-PD-1 antibody in PDAC, we used the hemispleen mouse model for liver metastases described above. This model accurately induces the expression of HA as is seen in spontaneously formed primary PDAC tumors[9, 21, 23]. We have previously used this model to demonstrate the effect of PEGPH20 on degrading extracellular HA in the stroma of the tumors formed in this hemispleen liver metastasis model. In the present study, following tumor implantation, mice with liver metastases were treated with PEGPH20, FAKi, and anti-PD-1 antibody for two weeks and sacrificed on POD16 for collection of TILs and IHC analysis. (Figure 1A). We found that PEGPH20 degraded HA in the stroma of liver metastases efficiently in combination with FAKi or both FAKi and anti-PD-1 antibody (Figure 1B). We then examined the expression of pFAK, Tyr397, the target of FAKi, in the same liver metastases from above treated mice. Previously, it was shown that FAKi modulates the TME of PDAC by inhibiting pFAK in tumor cells[11]. However, we found pFAK expression in multiple cell types in the stroma of PDAC (Supplemental Figure S1A) by multiplex IHC [28]. Due to lack of multiplex IHC for murine FAK, we quantified pFAK expression in cells with different sizes including smaller sizes (lowest tertile) in the range of those of lymphocytes, medium sizes (middle tertile) in the range of those of KPC tumor cells, and larger sizes (highest tertile) in the range of myeloid cells and fibroblasts (Figure 1C). We found that FAKi in different combination treatments decreased the pFAK expression modestly by 34.45%-58.36% in cells of all different sizes. Expression of pFAK was significantly more decreased in cells at a medium to larger size, which appeared to be myeloid cells and fibroblasts by morphology, in mice treated with the double or triple combinations containing FAKi and anti-PD-1 antibody compared to the double combination containing PEGPH20 and FAKi (Figure 1D). This suggests that FAKi in combination with anti-PD-1 antibody may preferentially target myeloid cells and fibroblasts, although further validation with multiplex IHC is needed.

We and others have shown that the combination of FAKi and anti-PD-1 antibody significantly improved survival in liver metastasis mice comparing to FAKi alone (Supplemental Figure S1B). However, the survival benefit of adding FAKi to anti-PD-1 treatment was modest in this mouse model with a large liver metastasis burden even though the treatment of FAKi and anti-PD-1 antibody was initiated on POD7. We, therefore,

hypothesized that the role of PEGPH20 in targeting the extracellular matrix protein HA, may synergize with the stromal cell-targeting effect of FAKi to potentiate the antitumor activity of anti-PD-1 antibody. Thus, we examined the antitumor activity of the triple combination of PEGPH20, FAKi and anti-PD-1 antibody in the liver metastasis model. We used a slower growing subclone of KPC tumor cells ($5x10^5$ cells per hemispleen) in this experiment. To avoid the effect of PEGPH20 on tumor establishment, PEGPH20 was administered on POD6 and continued BIW. FAKi and anti-PD-1 antibody treatment were also initiated at this time. Mice were followed until survival endpoints were met or the end of the experiment on POD90 (Figure 1A). The triple combination of FAKi, PEGPH20 and anti-PD-1 antibody resulted in a significantly improved survival of mice comparing to FAKi alone, or FAKi-based combinations with anti-PD-1 antibody or PEGPH20 (Figure 1E). We did not observe the improved survival in this slower growing subclone of KPC tumor cell line with the dual combination of FAKi and anti-PD-1 antibody compared to FAKi alone. This was possibly due to lack of a tumor-intrinsic effect of FAKi on the slower growing tumor cells. Taken together, our results support targeting the extracellular HA to enhance the tumor-extrinsic effect of FAKi and anti-PD-1 antibody in PDAC.

Adding PEGPH20 to the combination of FAKi and anti-PD-1 antibody significantly enhances effector T-cell infiltration and function

We next examined the immune-mediated mechanism underlying antitumor response to the triple combination of PEGPH20, FAKi and anti-PD-1 antibody. Previously, the combination of FAKi and anti-PD-1 antibody was shown to enhance the effector T-cell infiltration in PDAC[11]. We demonstrated that PEGPH20 enhances the $CD8^+$ T-cell infiltration and skews the tumor-infiltrating $CD8^+$ T-cells from naïve T-cells (Tnaïve) to Tem[9]. Therefore, we examined the combined effect of PEGPH20 and FAKi on effector T-cells. Following the hemispleen procedure tumor-bearing mice were treated starting POD6 and sacrificed POD16 for harvest of diffuse liver metastases and FACS analysis of TILs. We found that adding PEGPH20 to FAKi and anti-PD-1 antibody significantly increased the number of $CD3^+CD8^+$ T-cells (Figure 2A), but not $CD3^+CD4^+$ T-cells (Figure 2B), as compared to the dual combinations of FAKi and anti-PD-1 antibody, or FAKi and PEGPH20. Interestingly, adding PEGPH20 modestly decreased $CD4^+$ T-cells, albeit in a statistically significant manner. We further assessed the subtypes of $CD8^+$ T-cells, employing combinations of surface markers: $CD8^+CD44^-CD62L^+CCR7^+$ for Tnaïve, $CD8^+CD44^+CD62L^+CCR7^+$ for central memory T-cells (Tcm), and $CD8^+CD44^+CD62L^-CCR7^-$ for Tem as previously described[9] (Supplemental Figure S2A). As anticipated, the absolute numbers of Tnaïve, Tcm and Tem, were all significantly increased by adding PEGPH20 to the treatment of FAKi and anti-PD-1 antibody, likely as a result of overall increased infiltration of total $CD8^+$ T-cells (Supplemental Figure S2B-D). However, we found that the addition of PEGPH20 to combination FAKi and anti-PD-1 antibody led to a significant decrease in the percentage of the Tnaïve subpopulation, did not significantly alter the Tcm subpopulation, but significantly increased the percentage of the Tem subpopulation within the $CD8^+$ T-cell population (Figure 2C-E). Although the dual combination of FAKi and anti-PD-1 antibody also increased the percentage of Tem significantly comparing to untreated group, this experiment did not tell whether this is a contribution from FAKi or anti-PD-1 antibody.

Thus, we attempted to understand, among the effector T-cell signals, which were activated by the addition of PEGPH20 to the combination of FAKi and anti-PD-1 antibody. To this end, we performed RNA sequencing on $CD8^+$ T-cells isolated from TILs of dissected PDAC tumors from mice treated with dual or triple combinations of FAKi, PEGPH20 and/or anti-PD-1 antibody. We performed transcriptomic RNA expression analysis and selected differentially expressed genes that are enriched in the effector T-cell pathways and involved in effector T-cell activation and differentiation. As anticipated, there was low RNA expression with either $CD8^+$ T-cell effector or activation markers among the untreated, FAKi alone or FAKi with PEGPH20 treatment groups (Figure 2F). However, we found that: *CD69, CD27* and *IL7R*, whose gene products are associated with T-cell activation and differentiation, *IL2RA, IL2RG, TNFR1* and *IFNGR1*, whose gene products are associated with the type I cytokine response of $CD8^+$ T-cells, *PRF1, GZMK* and *GZMC*, whose gene products are associated with effector T-cell cytotoxicity, were upregulated in TILs from mice treated with the dual combination of FAKi and anti-PD-1 antibody compared to those from untreated mice, mice treated with FAKi alone, or mice treated with other dual combinations. Most of these genes continued to be upregulated in $CD8^+$ TILs from mice treated with triple combination of PEGPH20, FAKi and anti-PD-1 antibody. However, more genes associated with the effector T-cell cytotoxic function such as *IFNG, IFNGR2, GZMF*, and *GZMN*, were further upregulated with adding PEGPH20 to the combination of FAKi and anti-PD-1 therapy (Figure 2F), supporting a strong role of HA degradation in enhancing effector T-cell functions.

FAKi-based combination therapies alter CD8+ T-cell metabolism indirectly through upregulation of the chemokines from CAFs

Thus, we further explored the underlying mechanism of how combinatorial therapy with FAKi and PEGPH20 can enhance the functions of effector T-cells. We attempted to understand how FAKi modulates effector T-cell function. While we isolated tumor-infiltrating $CD8^+$ T-cells from above tumors (Figure 2F), we also used anti-FAP antibody conjugated magnetic beads to isolate FAP^+ cells, known to be mainly CAF[29]. RNA was extracted, followed by RNA sequencing analysis. Gene signatures of inflammatory CAFs (iCAF), myofibroblast CAFs (myCAF), or antigen-presenting CAFs (apCAF), particularly the top signature genes described previously[30, 31], were analyzed in isolated FAP^+ cells. iCAF and myCAF genes were upregulated in FAP^+ cells from mice treated by FAKi alone compared to untreated tumors, but were downregulated by the triple combination of FAKi, PEGPH20 and anti-PD-1 antibody (Supplemental Figure S3A) to levels comparable untreated mice. Overall, CAF heterogeneity was maintained in all treatment groups.

A recent study showed that genetic depletion of FAK from CAF results in upregulation of multiple metabolic pathways in tumor cells through a paracrine mechanism[32]. We thus hypothesized that pharmacological inhibition of FAK would lead to similar metabolism changes in both tumor cells and T-cells as the effect is mediated by a paracrine mechanism. Among the cytokine genes that were upregulated by genetic depletion of FAK in CAFs and that were thought to regulate tumor cell metabolism, we found that the gene products of *CCL6, CCL11, CCL12* and *pentraxin-3* may also modulate T-cells[32]. These genes were also upregulated in FAP^+ CAFs from mice treated with FAKi. However, after the addition

of PEGPH20 to the combination of FAKi and anti-PD-1 antibody, *CCL12* was the only chemokine gene among these appreciably upregulated (Figure 3A). CCL12 is a ligand of CCR2, which is mainly expressed in the bone marrow derived monocytes, but also expressed in $CD8^+$ effector T-cells and crucial for Th1 immune responses[33]. Mouse CCL12 does not have a human homolog. Therefore, other chemokines may have substituted the role of CCL12 in human PDAC. As Figure 2E showed that the Tem infiltration was enhanced by the triple combination of PEGPH20, anti-PD-1 and FAKi, we examined the expression of the Tem trafficking factor, CXCL9[34]. We found that CXCL9 was upregulated in the FAKi alone treated group and significantly in the group treated by FAKi-based triple combination with both anti-PD-1 antibody and PEGPH20 (Supplemental Figure S3B). In this study, we are not able to discern which CAF subtypes express CXCL9. It remains interesting to examine the expression of CXCL9 in the subtypes of CAF through a future single cell analysis. We further examined the metabolic pathways in the above RNA sequencing results of $CD8^+$ T-cells. These results showed that metabolic pathways previously known to be modulated in tumor cells as a result of FAK depletion in CAFs, including glycosylation, glycogen biosynthesis, negative regulation of protein catabolism and fatty acid biosynthesis, were upregulated by FAKi treatment, and further upregulated by FAKi based dual combinations with either PEGPH20 or anti-PD-1 antibody. Most strikingly, these pathways showed remarkable degrees of upregulation in isolated $CD8^+$ cells from triple combination PEGPH20, FAKi and anti-PD-1 antibody treated mice (Figure 3B). Thus, our data suggest that FAKi-based combination therapies may activate the effector T-cell functions by regulating T-cell metabolism indirectly through upregulation of the chemokines from CAFs.

Addition of PEGPH20 to FAKi and anti-PD-1 antibody more specifically decreased granulocytes and granulocytic-MDSCs in PDAC

Next, we attempted to elucidate how PEGPH20 in combination with FAKi and anti-PD-1 antibody modulates the effector T-cell function. We have previously shown that targeting the ECM by PEGPH20-mediated HA reduction modulates myeloid cells[9]. We thus analyzed myeloid cells from the liver metastases in the KPC hemispleen mouse model following treatment with FAKi, PEGPH20 and anti-PD-1 antibody, tumor bearing mice were sacrificed on Day 16, and livers with diffuse metastases were harvested for FACS analysis (Supplemental Figure S4A). We found that the addition of PEGPH20 to FAKi and anti-PD-1 antibody, significantly decreased the myeloid cell percentage among total TILs as compared to dual combinations of FAKi and PEGPH20 or FAKi and anti-PD-1 antibody (Figure 4A). We subsequently evaluated tumor associated granulocytes, MDSCs and TAMs. The addition of PEGPH20 to FAKi and anti-PD-1 antibody therapy led to a large and statistically significant decrease in the percentages of $CD3^-C11b^+Ly6G^+$ granulocytes (Figure 4B) and $CD3^-C11b^+$ $Ly6C^{Lo}Ly6G^+$ polymorphonuclear (Granulocytic) G-MDSCs (Figure 4C) among TILs as compared to the dual combinations of FAKi with PEGPH20 or with anti-PD-1 therapy. In contrast, although the addition of PEGPH20 to FAKi and anti-PD-1 antibody therapy decreased the percentages of $CD3^-CD11b^+Ly6^{Hi}Ly6G^-$ monocytic M-MDSCs (Figure 4D) and $CD3^-C11b^+F480^+Ly6G^-$ TAMs (Figure 4E) among TILs as compared to the dual combinations of FAKi with PEGPH20 or with anti-PD-1 therapy in a statistically significant manner, the level of decrease was quite modest. Although the

absolute numbers of these myeloid cell subtypes or their percentages among the total CD11b cells trended somewhat differently comparing to their percentages among all TILs, the results support that addition of PEGPH20 to FAKi and anti-PD-1 antibody more specifically decreased granulocytes and G-MDSCs comparing to the dual combination of FAKi and anti-PD-1 antibody (Supplemental Figure S4B-F). Therefore, this study has advanced our knowledge on the role of HA degradation in PDAC from previously being recognized in myeloid cells[9] to now being known more specifically in granulocytic myeloid cells, including G-MDSC.

Addition of PEGPH20 to FAKi and anti-PD-1 antibody decreases CXCR4$^+$ myeloid cells, particularly CXCR4$^+$ granulocytes and G-MDSC

We have previously shown that targeting PEGPH20 in combination with immunotherapy modulates the CXCL12/CXCR4/CCR7 immunosuppressive signaling axis through multiple cell types in the TME of PDAC including CAFs, myeloid cells and CD8$^+$ T-cells[9]. Therefore, we examined in the above FACS analysis of TILs to understand whether addition of PEGPH20 to FAKi and anti-PD-1 antibody would specifically regulate CXCR4$^+$ granulocytes. While we did not note a statistically significant difference in the percentage of CXCR4$^+$ myeloid cells among total TILs between different treatment groups, we appreciated a notable decreasing trend after the addition of PEGPH20 to FAKi and anti-PD-1 antibody (Figure 5A). We also found that the addition of PEGPH20 to FAKi and anti-PD-1 antibody significantly decreased the percentage of CXCR4$^+$ granulocytes (Figure 5B) and CXCR4$^+$ G-MDSCs (Figure 5C) among total granulocytes and G-MDSCs, respectively, and significantly decreased the absolute numbers of CXCR4$^+$ granulocytes and CXCR4$^+$ G-MDSC (Supplemental Figure S5). However, there was no significant difference in CXCR4$^+$ M-MDSCs and CXCR4$^+$ TAMs (Figure 5D&E) among their respective myeloid cell subtypes when comparing the triple combination treatment group and the dual combination groups of FAKi with PEGPH20 or with anti-PD-1 antibody. Although the absolute numbers of CXCR4$^+$ M-MDSCs and CXCR4$^+$ TAMs in the triple combination treatment group were decreased compared to the dual combination group of FAKi and anti-PD-1 antibody, they were at similar levels as those in the untreated group. Taken together, these results suggest that the addition of PEGPH20 to FAKi and anti-PD-1 antibody decreases CXCR4$^+$ myeloid cells, particularly CXCR4$^+$ granulocytes and G-MDSCs. These results are also consistent with the observation from the RNA sequencing analysis of FAP$^+$ CAFs showing that the gene expression of CXCL12, ligand of CXCR4, is increased by FAKi alone, but were brought down by the combination treatment with anti-PD-1 antibody, PEGPH20, or both anti-PD-1 antibody and PEGPH20 (Supplemental Figure S3B).

Combination of anti-CXCR4 antibody, anti-PD-1 antibody and FAKi prolongs survival and reduces the development of metastasis

Above results support the testing of the combination of PEGPH20, FAKi and anti-PD-1 antibody in the clinical trials of PDAC. As PEGPH20 is currently not in clinical development, we tested whether PEGPH20 can be replaced by directly targeting CXCR4 in this combinatorial therapy. The hemispleen liver metastasis model was again utilized as described above. Mice were treated with FAKi and anti-PD-1 antibody at the same dose and schedule as in Figure 1E, together with anti-CXCR4 antibody at 10mg/kg given

BIW. In the first experiment, where mice were treated for 21 days, we noted a statistically more significant survival improvement with the triple combination of anti-CXCR4 antibody, FAKi and anti-PD-1 antibody than the double combination of FAKi and anti-PD-1 antibody compared to untreated group (Supplemental Figure S6A). In the repeated experiment to demonstrate a clear contribution of anti-CXCR4 antibody to the antitumoral activity of the triple combination, we used the slower growing subclone of the KPC tumor cell line as the one used in Figure 1E. In addition, the mice were treated with anti-CXCR4 antibody 10mg/kg BIW beyond 21 days until they either met the survival endpoint or until POD180. All survived mice were euthanized on POD180. On POD180, most of anti-CXC4 antibody-treated mice were still alive. Therefore, the formation of liver metastases was assessed as the efficacy endpoint. Mice were examined for liver metastases macroscopically and microscopically either when they were euthanized or found dead (Supplemental Figure S6B). The results showed that the triple combination of anti-CXCR4 antibody, anti-PD-1 antibody and FAKi led to a significant reduction in the rate of liver metastases, as compared to the dual combinations of FAKi and anti-PD-1 antibody or anti-CXCR4 with anti-PD-1 antibody (Figure 6).

Discussion:

Here for the first time, we demonstrate that the addition of PEGPH20 to FAKi and anti-PD-1 antibody enhances survival in a murine model of PDAC. The results support development of a combination immunotherapy targeting multiple components of the stroma. Targeting the tumor stroma via PEGPH20 in combination with FAKi and anti-PD-1 antibody further enhances effector T-cell infiltratation, as well as cytokine response for effector T-cell function and activation. We also suggest that FAKi regulates T-cell metabolism by targeting CAFs via CCL12. The mechanism of action of PEGPH20 in this combination in the absence of the GVAX vaccine appears to be similar to our prior observation of PEGPH20 in combination with GVAX; executed by decreasing immunosuppresive myeloid cells and enhancing effector T-cell infiltration. Thus, PEGPH20 and FAKi provide dual stroma targeting effects (Figure 7), leading to enhanced effector T-cell priming. Therefore, this combinatorial therapy serves as an alternative therapautic strategy to our previously developed vaccine-based combination immunotherapy approaches. This current study further reveals the primary mechanism of action of the combination of PEGPH20, FAKi, and anti-PD-1 antibody on the CXCR4-expressing granulocytic myeloid cells. Lastly, our results support further testing of directly targeting CXCR4 in combination with FAKi and anti-PD-1 antibody in treating PDAC in preclinical and clinical studies.

In this study we found that the addition of PEGPH20 to FAKi and anti-PD-1 antibody significantly decreased stromal HA density and decreased phosphorylated FAK expression in cell types likely to be tumor epithelial cells, CAFs and myeloid cells. Cell type categorization was based on cell morphology and cell size. We recognize that because this approach was based on a cutoff for cell size, it cannot differentiate among cells within the same size range. Thus, in the future we will investigate whether FAKi impacts FAK expression in specific cell types utilizing specific cell type biomarker colocalization. Previously, a tumor-intrinsic FAK signaling was considered to be important for modulating the TME of PDAC[11]. In this study, we found that FAK is expressed in multiple cell types in

the TME of human PDACs. Therefore, the observed effects of FAK inhibition in this study could result from a direct inhibition on CAFs and myeloid cells. However, future studies are warranted to rule out the FAK kinase-independent activity of VS-4718.

The dual combination of anti-PD-1 antibody and FAKi increases activation signals in *CD27, CD69* and *TNFR1(TNFRSAF1A)*, which can be appreciably increased in the naïve T-cell population[35]. With the addition of PEGPH20 to FAKi and anti-PD1, these signals were downregulated. Conversely, we note a significant upregulation of more cytotoxic cytokine expression including *IFNG, IFNGR2, GZMF*, and *GZMN*, further reflective of an enhanced effector T-cell function. These results are consistent with the observed increase in the Tem cell phenotype seen after the triple combination therapy of FAKi, PEGPH20, and anti-PD-1 antibody. In the future, it is warranted to validate the increase in the cytotoxic activity of T-cells with a functional assay such as measuring the production of IFN-γ.

Previously, it has been shown that FAK depletion in CAFs results in upregulation of cytokines such as CCL6, CCL11, CCL12 and pentraxin-3 (PTX3)[32]. In our investigation, we also found that with FAKi treatment alone, similar genes were upregulated in CAFs and anticipated to alter the tumor cell metabolism in favor of tumor growth. However, when combining PEGPH20 and anti-PD-1 antibody to FAKi, only *CCL12* remained upregulated. This preferential upregulation of CCL12 may specifically mediate immune cell metabolic changes. CCL12 is a ligand of CCR2, which is mainly expressed on bone marrow derived monocytes[36, 37], but also on activated effector T-cells[38]. We anticipated that CCL12 would recruit more monocytic myeloid cells to the tumors. However, the percentages of M-MDSC and TAM among TILs were not increased in tumors from the triple combination group. In contrast, we observed the upregulation of gene signatures of multiple metabolic pathways that favor an enhanced effector T-cell function[32]. It remains interesting to examine which CAF subtype is responsible for the chemokine expression that leads to altered T cell metabolism.

In this study, we confirmed the role of PEGPH20 in suppressing the CXCR4/CCR7 axis in myeloid cells, particularly, the granulocytic myeloid cells. This study thus highlighted the importance of granulocytes in the TME of PDAC. For the first time, we linked HA, an ECM protein to the CXCR4-expressing immunosuppressive granulocytes in PDAC. Although we did not investigate specifically, we anticipate that HA modulates CXCR4-expressing granulocytes via CXCL12, the ligand of CXCR4 which is mainly expressed by CAFs. Therefore, the combination of PEGPH20 and FAKi targets the stroma/CAFs through two pathways, possibly one through the CXCL12/CXCR4/CCR7 axis and the other through the CCL12/CCR2 axis. Although the advantage of targeting dual stromal pathways remains to be assessed, it is conceivable that this dual stroma pathway targeting approach may help overcome the tumor's compensatory resistance mechanisms. For example, FAK inhibition in CAFs results in upregulation of cytokines that may induce multiple immunosuppressive signals and alter the tumor cell metabolism, whereas targeting CAFs, with both FAKi and PEGPH20 only induces CCL12 while also suppressing CXCL12.

As PEGPH20 is currently not in clinical development, we explored the possibility of replacing PEGPH20 with a CXCR4 targeting agent in the combination treatment with FAKi

and anti-PD-1 antibody. In this study, three-week treatment of the triple combination of anti-CXCR4 antibody, anti-PD-1 antibody and FAKi prolonged survival more significantly than the dual combination of anti-PD-1 antibody and FAKi compared to the untreated mice, although there was only a non-significant trend of survival improvement with the triple combination compared to the dual combination. Nevertheless, when the treatment of anti-CXCR4 antibody was prolonged, the triple combination with anti-CXCR4 antibody significantly reduced the rate of metastasis compared to dual combinations. Therefore, this study supports further testing the combination of a more potent CXCR4 targeting agent, FAKi and anti-PD-1 antibody in future preclinical studies and clinical trials of PDAC.

Supplementary Material

Refer to Web version on PubMed Central for supplementary material.

Grant Support:

This work was supported in part by a research grant from Halozyme, independent from Verastem Oncology and Bristol-Meyer Squibb, and a NIH P01 grant P01CA247886. VS-4718 was provided by Verastem Oncology; PEGPH20 was provided by Halozyme; and anti-CXCR4 antibody provided by Bristol-Meyer Squibb via the II-ON program, all independently. The opinions expressed in this paper are those of the authors and do not necessarily represent those of Verastem Oncology, Halozyme or Bristol-Meyer Squibb. AB is supported by an NIH T32 CA126607 grant. AO is supported by an NIH grant K08 CA259456 and a Conquer Cancer Foundation ASCO Career Development Award. LZ is supported by an NIH grant R01 CA169702, an NIH grant R01 CA197296, an NIH grant P01CA247886, an NIH SPORE grant P50 CA062924, and an NIH Cancer Center Support Grant P30 CA006973.

Abbreviations:

PDAC	Pancreatic ductal adenocarcinoma
TME	tumor microenvironment
HA	hyaluronic acid
CAF	cancer-associated-fibroblast
GVAX	GM-CSF secreting allogenic tumor cell vaccine
FAK	focal adhesion kinase
anti-PD1	anti-PD-1 antibody
PEGPH20	PEGylated recombinant human hyaluronidase
ECM	extracellular matrix
MDSC	myeloid-derived suppressor cell
TAM	tumor associated macrophages
Treg	regulatory T-cell
FAKi	FAK inhibition
Tern	effector memory $CD8^+$ T-cell

PBS	phosphate buffered saline
BIW	semiweekly/biweekly
POD	Post-operative day
BID	twice daily
TIL	tumor-infiltrating leukocytes
FAP	fibroblast activation protein
IHC	Immunohistochemistry
pFAK	phosphorylated FAK
Tnaïve	naïve T-cell
Tcm	central memory T-cell
iCAF	inflammatory CAF
myCAF	myofibroblast CAF
apCAF	antigen-presenting CAF
G-MDSC	granulocytic MDSC
M-MDSC	monocytic MDSC

References:

1. Siegel RL, Miller KD, Jemal A. Cancer statistics, 2020. CA Cancer J Clin 2020;70:7–30. [PubMed: 31912902]
2. Osipov A, Murphy A, Zheng L. From immune checkpoints to vaccines: The past, present and future of cancer immunotherapy. Volume 143: Academic Press, 2019:63–144.
3. Laklai H, Miroshnikova YA, Pickup MW, et al. Genotype tunes pancreatic ductal adenocarcinoma tissue tension to induce matricellular fibrosis and tumor progression. Nat Med 2016;22:497–505. [PubMed: 27089513]
4. Sato N, Kohi S, Hirata K, et al. Role of hyaluronan in pancreatic cancer biology and therapy: Once again in the spotlight. Cancer Sci 2016;107:569–75. [PubMed: 26918382]
5. Zhang L, Li J, Zong L, et al. Reactive Oxygen Species and Targeted Therapy for Pancreatic Cancer. Oxid Med Cell Longev 2016;2016:1616781. [PubMed: 26881012]
6. Arcucci A, Ruocco MR, Granato G, et al. Cancer: An Oxidative Crosstalk between Solid Tumor Cells and Cancer Associated Fibroblasts. Biomed Res Int 2016;2016:4502846. [PubMed: 27595103]
7. Liao Z, Chua D, Tan NS. Reactive oxygen species: a volatile driver of field cancerization and metastasis. Mol Cancer 2019;18:65. [PubMed: 30927919]
8. Thomas D, Radhakrishnan P. Tumor-stromal crosstalk in pancreatic cancer and tissue fibrosis. Mol Cancer 2019;18:14. [PubMed: 30665410]
9. Blair AB, Kim VM, Muth ST, et al. Dissecting the Stromal Signaling and Regulation of Myeloid Cells and Memory Effector T Cells in Pancreatic Cancer. Clin Cancer Res 2019;25:5351–5363. [PubMed: 31186314]

10. Ozdemir BC, Pentcheva-Hoang T, Carstens JL, et al. Depletion of carcinoma-associated fibroblasts and fibrosis induces immunosuppression and accelerates pancreas cancer with reduced survival. Cancer Cell 2014;25:719–34. [PubMed: 24856586]
11. Jiang H, Hegde S, Knolhoff BL, et al. Targeting focal adhesion kinase renders pancreatic cancers responsive to checkpoint immunotherapy. Nat Med 2016;22:851–60. [PubMed: 27376576]
12. Rhim AD, Oberstein PE, Thomas DH, et al. Stromal Elements Act to Restrain, Rather Than Support, Pancreatic Ductal Adenocarcinoma. Cancer Cell 2014;25:735–747. [PubMed: 24856585]
13. Hingorani SR. Phase Ib Study of PEGylated Recombinant Human Hyaluronidase and Gemcitabine in Patients with Advanced Pancreatic Cancer, 2016.
14. Jacobetz MA, Chan DS, Neesse A, et al. Hyaluronan impairs vascular function and drug delivery in a mouse model of pancreatic cancer. Gut 2013;62:112–20. [PubMed: 22466618]
15. Thompson CB, Shepard HM, O'Connor PM, et al. Enzymatic depletion of tumor hyaluronan induces antitumor responses in preclinical animal models. Mol Cancer Ther 2010;9:3052–64. [PubMed: 20978165]
16. Van Cutsem E, Tempero MA, Sigal D, et al. Randomized Phase III Trial of Pegvorhyaluronidase Alfa With Nab-Paclitaxel Plus Gemcitabine for Patients With Hyaluronan-High Metastatic Pancreatic Adenocarcinoma. J Clin Oncol 2020;38:3185–3194. [PubMed: 32706635]
17. Osipov A, Li K, Choi D, et al. The Implications of Focal Adhesion Kinase (FAK) on T-cell Populations in Immunotherapy Treated Pancreatic Ductal Adenocarcinoma (PDAC). Pancreas 2019;48:1503–1503.
18. Weis SM, Lim S-T, Lutu-Fuga KM, et al. Compensatory role for Pyk2 during angiogenesis in adult mice lacking endothelial cell FAK. Journal of Cell Biology 2008;181:43–50. [PubMed: 18391070]
19. Wang-Gillam A, Lockhart AC, Tan BR, et al. Phase I study of defactinib combined with pembrolizumab and gemcitabine in patients with advanced cancer. Journal of Clinical Oncology 2018;36:380–380.
20. Bockorny B, Semenisty V, Macarulla T, et al. BL-8040, a CXCR4 antagonist, in combination with pembrolizumab and chemotherapy for pancreatic cancer: the COMBAT trial. Nat Med 2020;26:878–885. [PubMed: 32451495]
21. Hingorani SR, Wang L, Multani AS, et al. Trp53R172H and KrasG12D cooperate to promote chromosomal instability and widely metastatic pancreatic ductal adenocarcinoma in mice. Cancer Cell 2005;7:469–83. [PubMed: 15894267]
22. Foley K, Rucki AA, Xiao Q, et al. Semaphorin 3D autocrine signaling mediates the metastatic role of annexin A2 in pancreatic cancer. Sci Signal 2015;8:ra77. [PubMed: 26243191]
23. Soares KC, Foley K, Olino K, et al. A preclinical murine model of hepatic metastases. J Vis Exp 2014:51677. [PubMed: 25285458]
24. Soares KC, Rucki AA, Wu AA, et al. PD-1/PD-L1 Blockade Together With Vaccine Therapy Facilitates Effector T-Cell Infiltration Into Pancreatic Tumors. Journal of Immunotherapy 2015;38:1–11. [PubMed: 25415283]
25. Jadin L, Huang L, Wei G, et al. Characterization of a novel recombinant hyaluronan binding protein for tissue hyaluronan detection. J Histochem Cytochem 2014;62:672–83. [PubMed: 24891594]
26. Keane FM, Yao TW, Seelk S, et al. Quantitation of fibroblast activation protein (FAP)-specific protease activity in mouse, baboon and human fluids and organs. FEBS Open Bio 2013;4:43–54.
27. Babicki S, Arndt D, Marcu A, et al. Heatmapper: web-enabled heat mapping for all. Nucleic Acids Research 2016;44:W147–W153. [PubMed: 27190236]
28. Tsujikawa T, Kumar S, Borkar RN, et al. Quantitative Multiplex Immunohistochemistry Reveals Myeloid-Inflamed Tumor-Immune Complexity Associated with Poor Prognosis. Cell Reports 2017;19:203–217. [PubMed: 28380359]
29. Xiao Q, Zhou D, Rucki AA, et al. Cancer-Associated Fibroblasts in Pancreatic Cancer Are Reprogrammed by Tumor-Induced Alterations in Genomic DNA Methylation. Cancer Res 2016;76:5395–404. [PubMed: 27496707]
30. Ohlund D, Handly-Santana A, Biffi G, et al. Distinct populations of inflammatory fibroblasts and myofibroblasts in pancreatic cancer. J Exp Med 2017;214:579–596. [PubMed: 28232471]

31. Biffi G, Oni TE, Spielman B, et al. IL1-Induced JAK/STAT Signaling Is Antagonized by TGFbeta to Shape CAF Heterogeneity in Pancreatic Ductal Adenocarcinoma. Cancer Discov 2019;9:282–301. [PubMed: 30366930]

32. Demircioglu F, Wang J, Candido J, et al. Cancer associated fibroblast FAK regulates malignant cell metabolism. Nat Commun 2020;11:1290. [PubMed: 32157087]

33. Lind L, Svensson A, Thorn K, et al. CD8(+) T cells in the central nervous system of mice with herpes simplex infection are highly activated and express high levels of CCR5 and CXCR3. J Neurovirol 2021;27:145–153. [PubMed: 33492607]

34. Mohan K, Ding Z, Hanly J, et al. IFN-gamma-inducible T cell alpha chemoattractant is a potent stimulator of normal human blood T lymphocyte transendothelial migration: differential regulation by IFN-gamma and TNF-alpha. J Immunol 2002;168:6420–8. [PubMed: 12055261]

35. Ding XL, Yang W, Shi XD, et al. TNF Receptor 1 Mediates Dendritic Cell Maturation and CD8 T Cell Response through Two Distinct Mechanisms. Journal of Immunology 2011;187:1184–1191.

36. Rho J, Takami M, Choi Y. Osteoimmunology: interactions of the immune and skeletal systems. Mol Cells 2004;17:1–9. [PubMed: 15055519]

37. Lim JK, Obara CJ, Rivollier A, et al. Chemokine Receptor Ccr2 Is Critical for Monocyte Accumulation and Survival in West Nile Virus Encephalitis. Journal of Immunology 2011;186:471–478.

38. Bakos E, Thaiss CA, Kramer MP, et al. CCR2 Regulates the Immune Response by Modulating the Interconversion and Function of Effector and Regulatory T Cells. J Immunol 2017;198:4659–4671. [PubMed: 28507030]

WHAT YOU NEED TO KNOW

Background and Context

Targeting multiple stromal components through both intracellular and extracellular mechanisms may overcome therapeutic resistance and enhance immunotherapy response in pancreatic adenocarcinoma.

New Findings

Stromal hyaluronan degradation combined with intracellular inhibition of focal adhesion kinase, and immunotherapy, decrease immunosuppressive myeloid cells, leading to increased T-cell infiltration through the CXCR4 pathway and improved murine survival.

Limitations

Specific changes in the tumor microenvironment by directly targeting CXCR4 and focal adhesion kinase are unknown.

Impact

Targeting intracellular and extracellular elements of pancreatic cancer stroma leads to synergistic enhancement of immunotherapy and further support direct targeting of CXCR4 in a combinatorial immunotherapeutic treatment strategy.

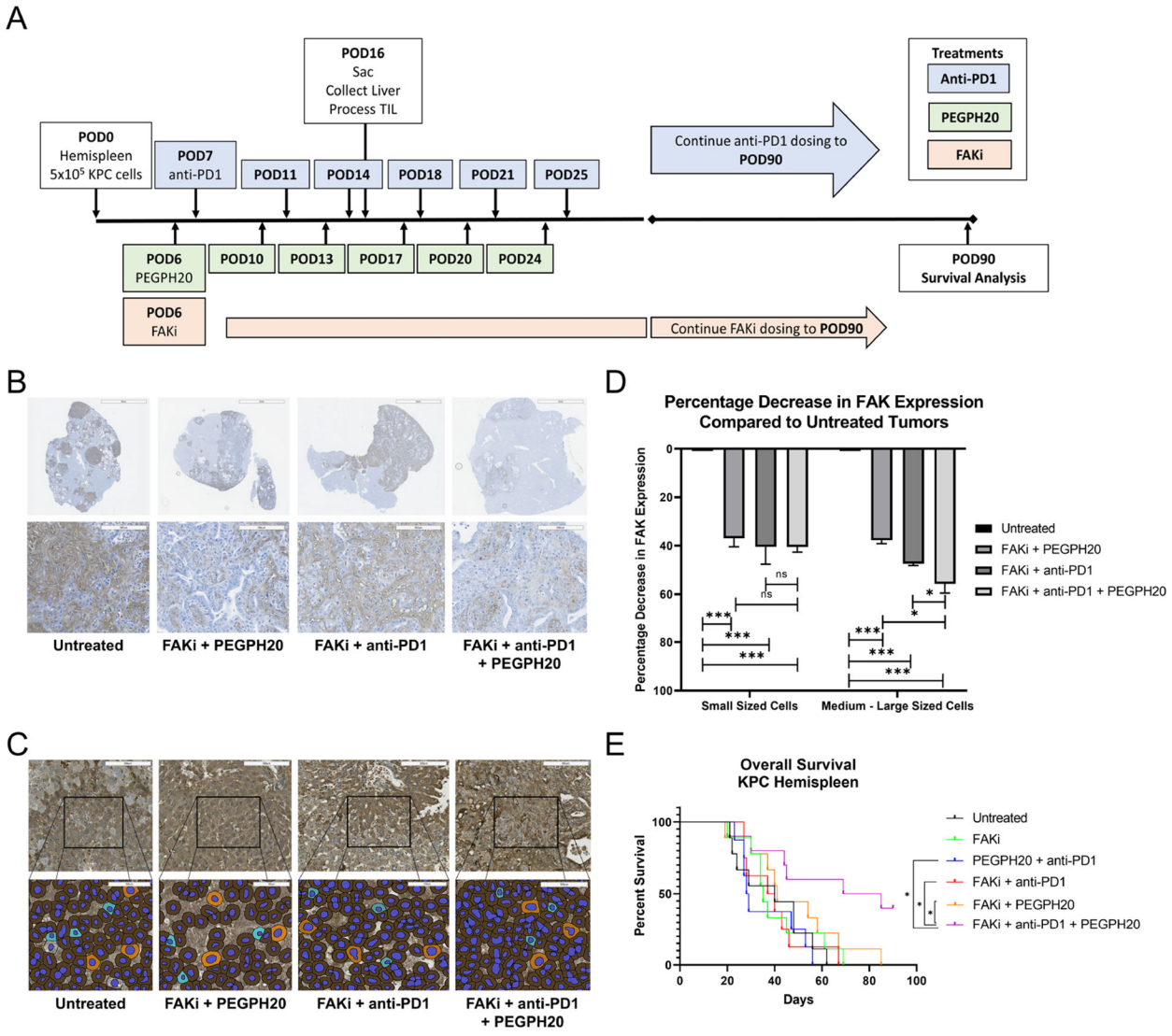

Figure 1: HA degradation and reduced FAK expression are associated with improved survival in PDAC bearing mice treated with PEGPH20, FAKi and anti-PD-1 antibody.

(A) The treatment schema of the liver metastasis model by PEGPH20, FAKi, anti-PD-1 antibody (anti-PD1), or their combinations. Mice were treated until POD90 or until survival endpoints were met. (**B**) IHC staining of HA and (**C**) pFAK of tumor bearing mice and corresponding treatments (n=3 per group). Representative medium to large sized cells circled in orange; small sized cells circled in blue using Halo software. (**D**) pFAK staining was quantified by the Halo software in small, medium, and large sized cells. Medium and large cell groups were combined. Treatment groups were compared by the 2-way ANOVA test. *p<0.05, **p<0.01, ***p<0.001, ns: not significant. (**E**). Kaplan–Meier survival curves of mice following tumor implantation (5 x 10^5 cells per mice) and treatments as described in (**A**). (n=10 per group). *p<0.05 by log-rank test. Data represent mean±SEM from one representative experiment. These experiments were repeated twice.

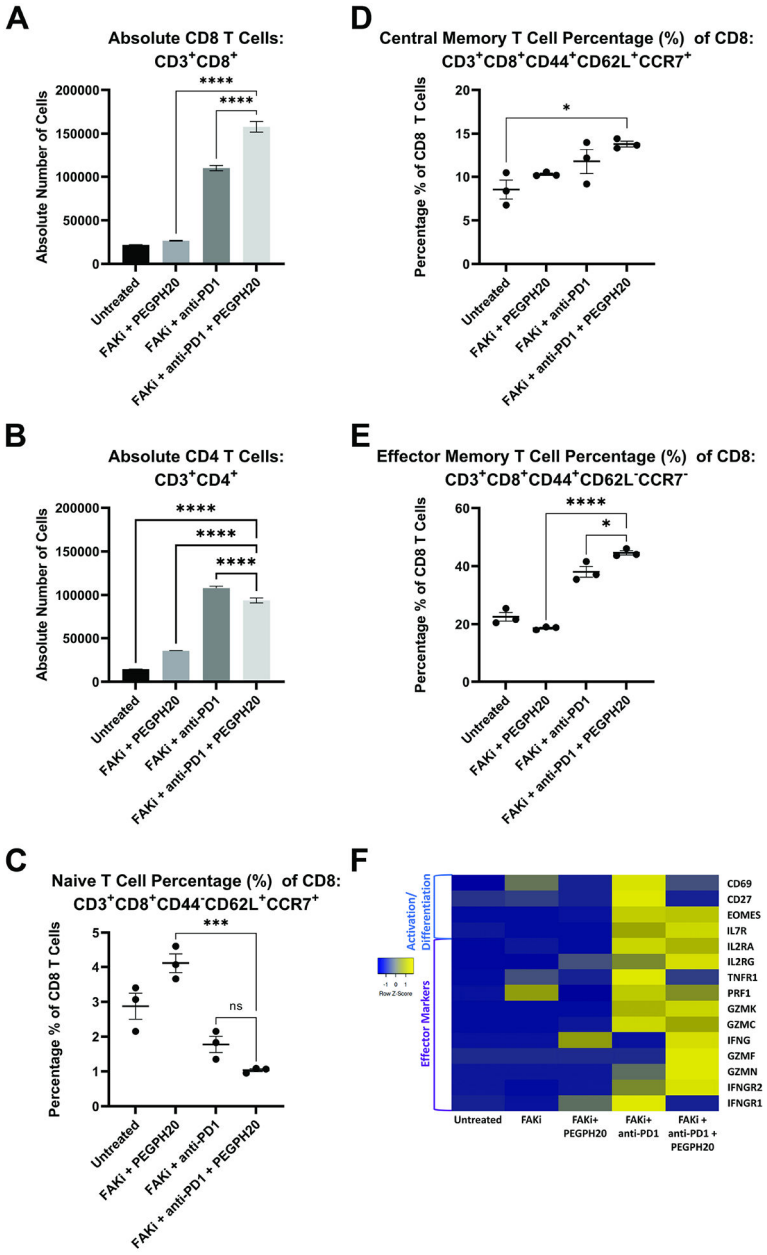

Figure 2: HA degradation with PEGPH20 in combination with FAKi and anti-PD-1 antibody increases T-cell infiltration and alters T-cell phenotype towards Tem cells.

Flow cytometry was performed on TILs isolated from individually processed diffusely metastatic livers of hemispleen mice. Total number of (**A**) live $CD3^+CD8^+$ T-cells and (**B**) $CD3^+CD4^+$ T-cells across indicated treatments. Percentages of (**C**) Tnaïve cells: $CD8^+CD44^-CD62L^+CCR7^+$, (**D**) Tem cells:$CD8^+CD44^+CD62L^+CCR7^+$ and (**E**) Tem cells:$CD8^+CD44^+CD62L^+CCR7^-$ among the $CD8^+$ T-cell population as quantified by flow cytometry analysis. Data represent mean±SEM from one representative experiment of 3 mice per treatment group analyzed individually and repeated by flow cytometry. *p<0.05, **p<0.01, ***p<0.001, ns: not significant, by 1-way ANOVA. (**F**) RNAseq heatmap

representing normalized expression of genes specific to T-cell activation/differentiation and effector function. T-cell

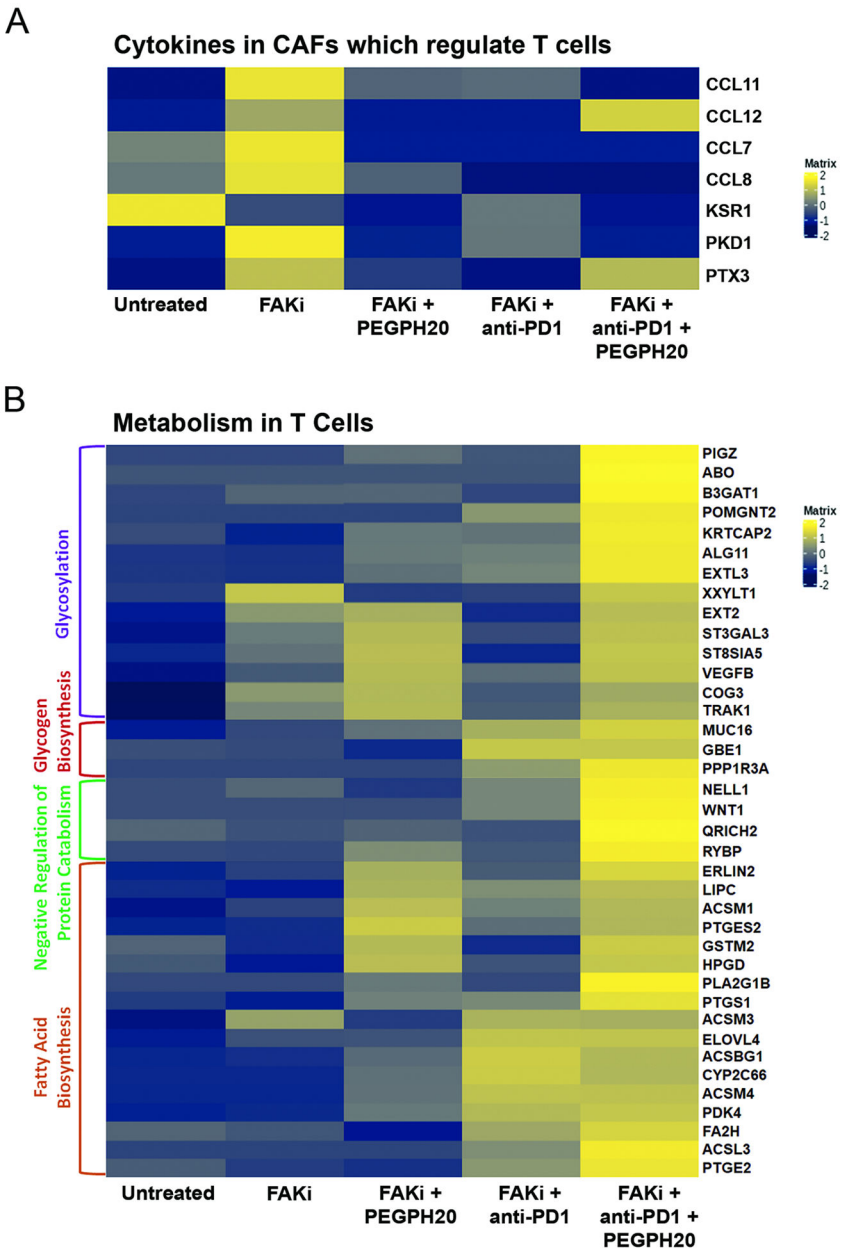

Figure 3: FAKi alter fibroblasts T-cell metabolism related cytokines and leads to changes in T-cell metabolism.

RNAseq was performed on isolated FAP$^+$ CAFs and CD8$^+$ T cells of tumor bearing mice. Comparative RNA expression of genes in (**A**) cytokines in CAF populations involved in T-cell metabolism and (**B**) T-cells involved in glycosylation, glycogen biosynthesis, negative regulation of protein catabolism and fatty acid biosynthesis across treatment groups as indicated. (n=3 mice per group, pooled)

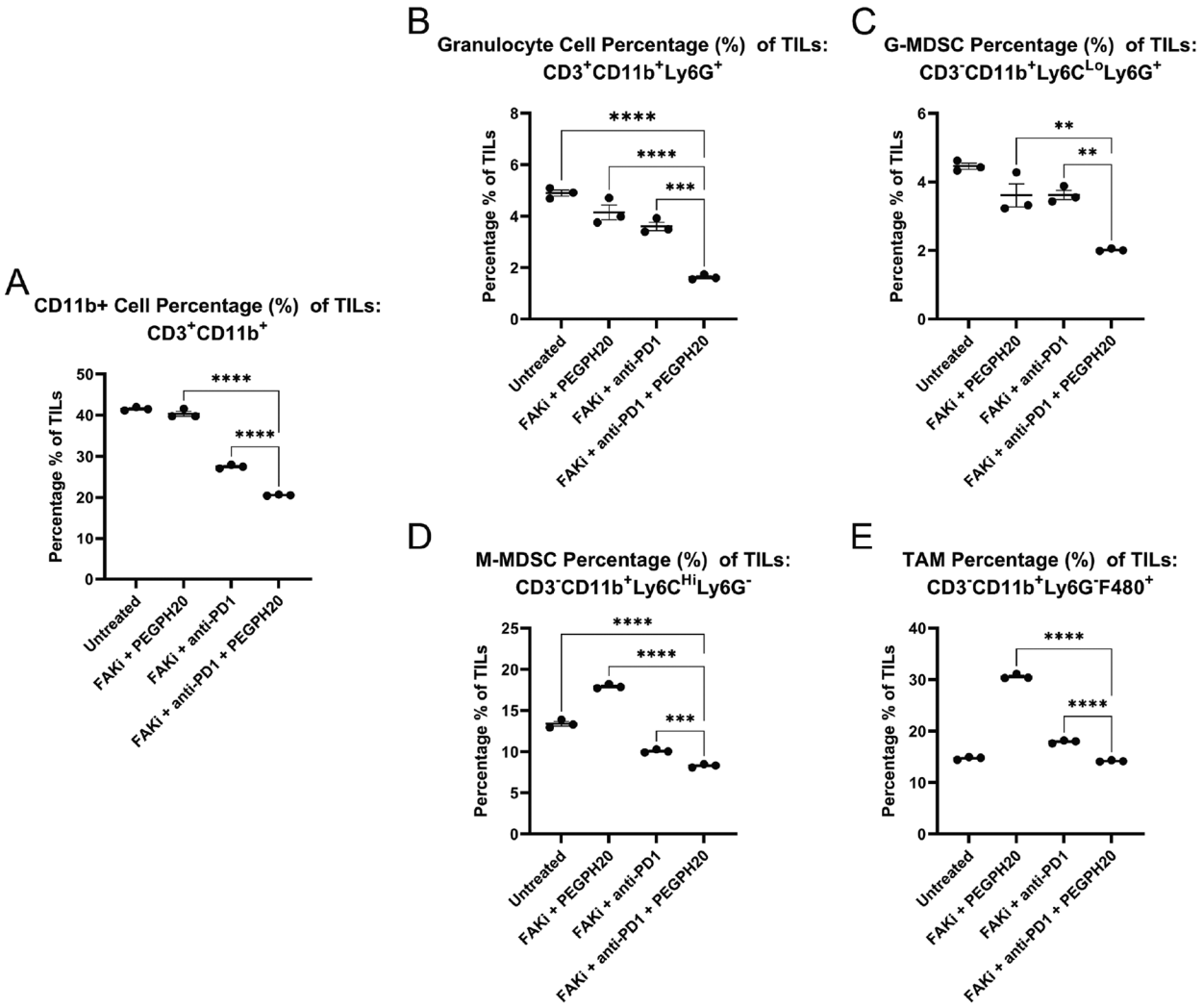

Figure 4: Stromal targeting of HA by PEGPH20 improves anti-PD-1 antibody modulation of myeloid cells, with specific reduction in granulocytes, G-MDSCs, and M-MDSCs.

Flow cytometry was performed on TILs isolated from individually processed diffusely metastatic livers of hemispleen mice. Percentage of (**A**) live $CD3^{-}CD11B^{+}$ cells, (**B**) granulocytes: $CD3^{-}CD11b^{+}Ly6G^{+}$, (**C**) G-MDSCs: $CD3^{-}CD11b^{+}Ly6C^{Lo}Ly6G^{+}$, (**D**) M-MDSC: $CD3^{-}CD11b^{+}Ly6C^{Hi}Ly6G^{-}$, and (**E**) TAM: $CD3^{-}C11b^{+}F480^{+}Ly6G^{-}$ among total TIL across treatment groups as indicated. Data represent mean ±SEM from one representative experiment of 3 mice per treatment group analyzed individually and repeated. *p<0.05, **p<0.01, ***p<0.001, ****p<0.0001, ns: not significant, by 1-way ANOVA.

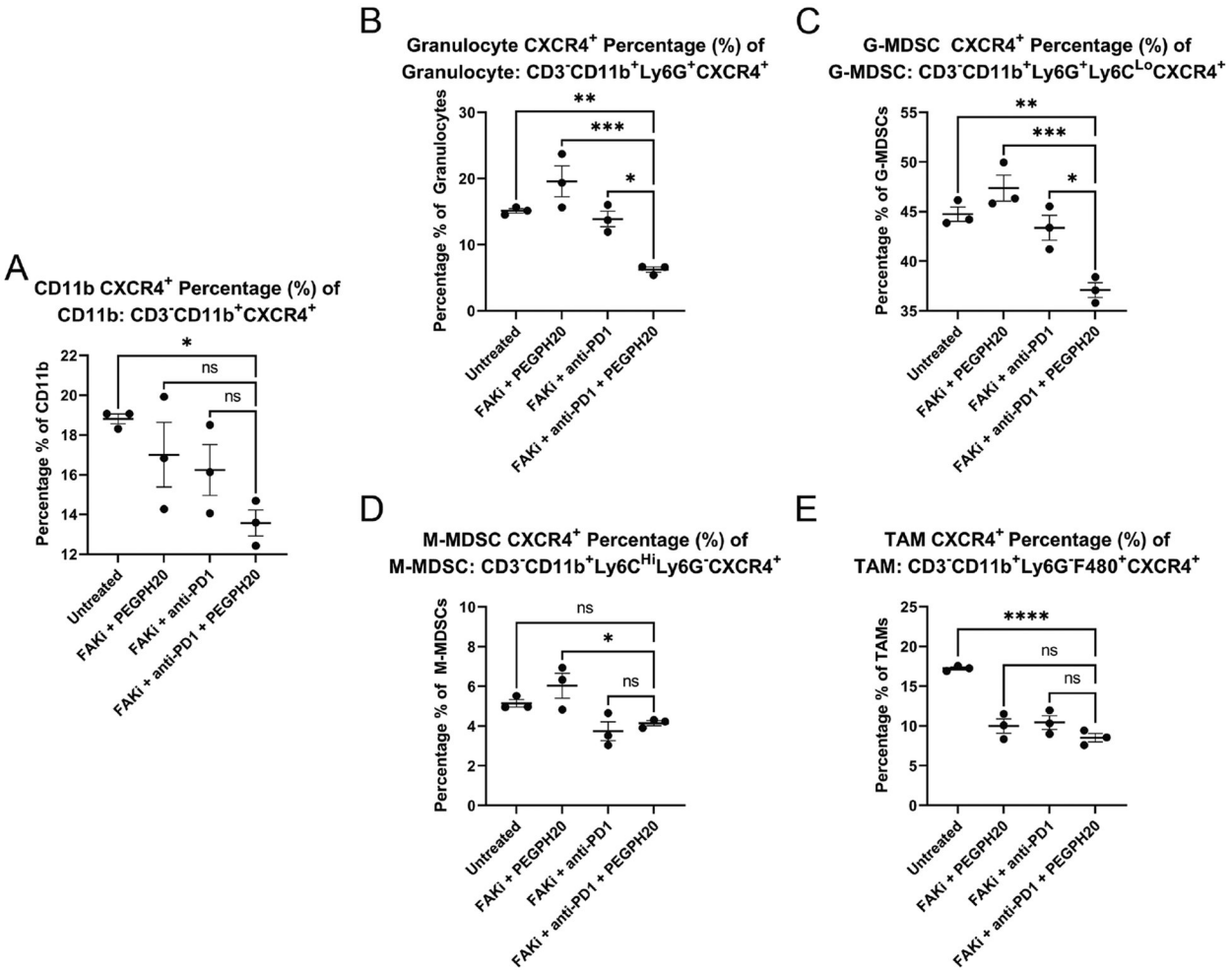

Figure 5: HA degradation with PEGPH20 in combination with anti-PD-1 antibody and FAKi decreases CXCR4 expression in myeloid cells, particularly in the CXCR4$^+$ granulocyte phenotype.

Flow cytometry was performed on TILs isolated from individually processed diffusely metastatic livers of hemispleen mice. Percentage of CXCR4$^+$ expression among representative myeloid phenotype: (**A**) live CD3$^-$CD11B$^+$ cells, (**B**) granulocytes:CD3$^-$CD11b$^+$Ly6G$^+$CXCR4$^+$, (**C**) G-MDSCs: CD3$^-$CD11b$^+$Ly6c^{Lo}Ly6G$^+$CXCR4$^+$, (**D**) M-MDSCs:CD3$^-$CD11b$^+$Ly6C^{HI}Ly6G$^-$CXCR4$^+$ and (**E**) TAM:CD3$^-$C11b$^+$Ly6G$^-$F480$^+$CXCR4$^+$ across treatment groups as indicated. Data represent mean±SEM from one representative experiment of 3 mice per treatment group analyzed individually and repeated. *p<0.05, **p<0.01, ***p<0.001, ****p<0.0001,ns: not significant, by 1-way ANOVA.

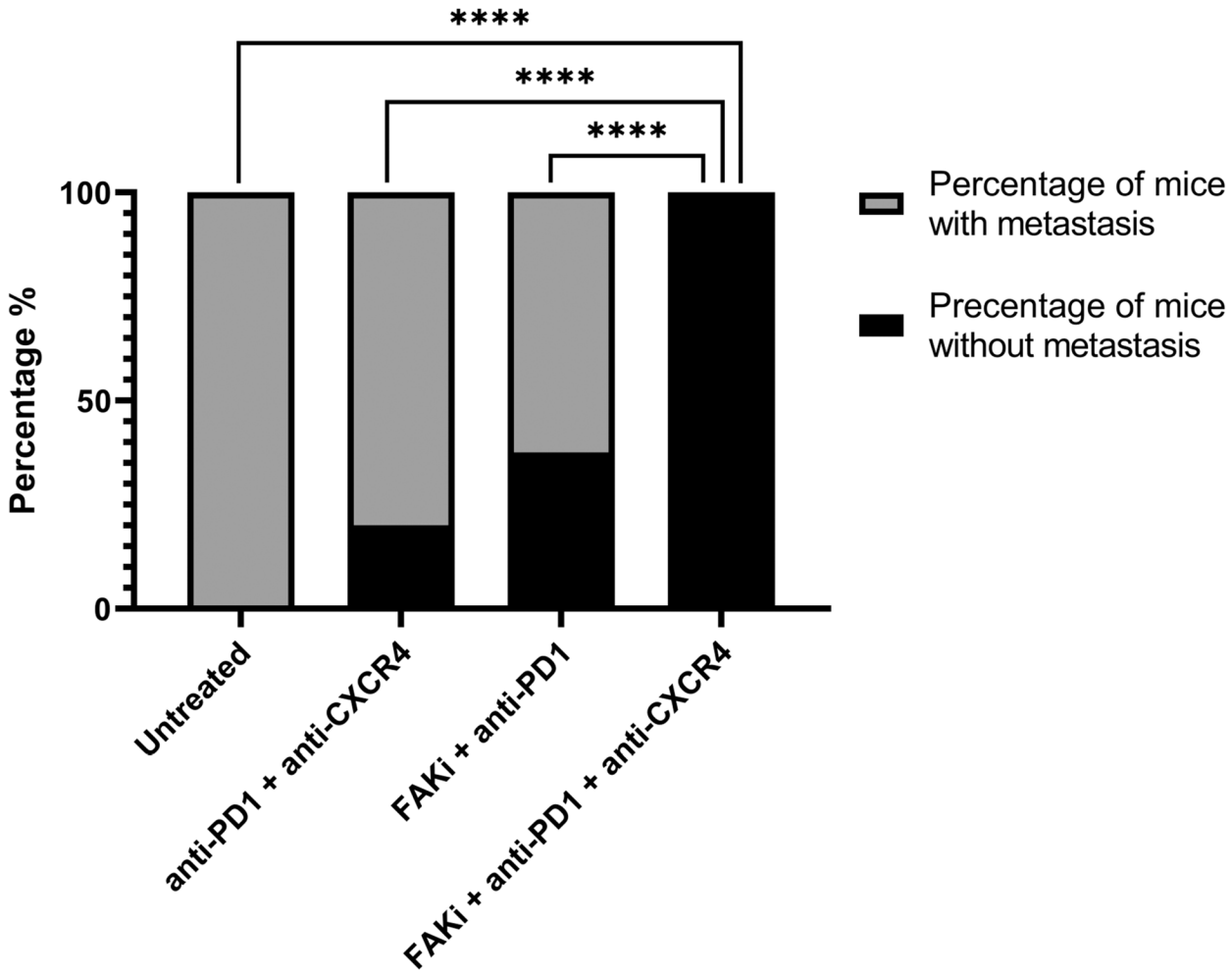

Figure 6: Anti-CXCR4 antibody combined with FAKi and anti-PD-1 antibody significantly decreases development of metastasis.

KPC tumors were implanted through the hemispleen procedure. Beginning on POD6, mice received 5mg/kg of anti-PD1 through IP injection BIW, 10mg/kg of anti-CXCR4 BIW and 50mg/kg of FAKi with oral gavage BID. for 90 days (n=10 mice per treatment group). The development of micrometastasis was compared among each treatment group using chi-square test. ****p<0.0001.

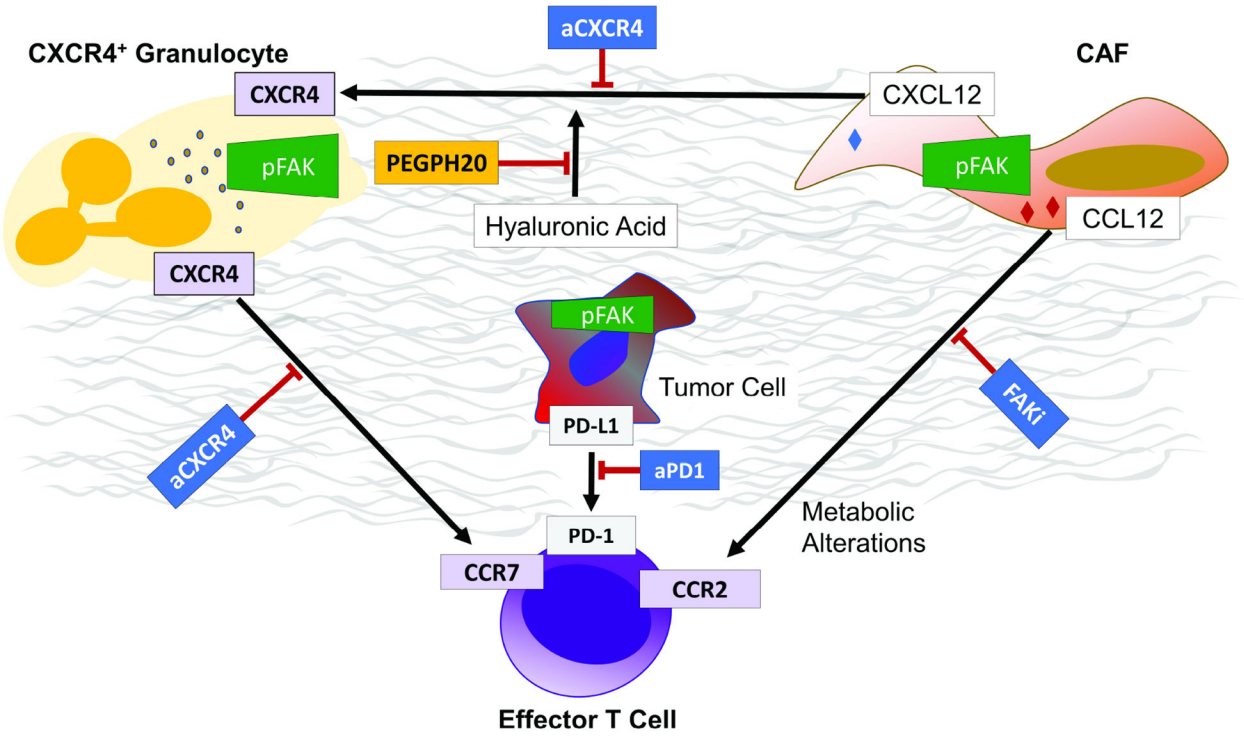

Figure 7: Working model of the mechanistic role of PEGPH20, FAKi and anti-CXCR4 in the TME of PDAC.

The pancreatic cancer TME is dense, fibrotic and contains both extracellular (HA) and intracellular (FAK) immunosuppressive elements leading to a lack of anti-tumor CD8 T-cells. FAKi alters the expression of T-cell modulating cytokines, in CAFs, like CCL12 and leads to changes in T-cell metabolism and increases in effector T-cells. CXCL12 expression is appreciated in CAFs within the stroma. Downstream CXCR4 expression, particularly among the myeloid granulocyte population, is diminished in targeting both the PEGPH20 and FAKi. PEGPH20 and FAKi target dual stroma aspects leading to stronger effector T-cell priming. Directly targeting CXCR4 in replacement of targeting PEGPH20, may lead to further T-cell priming and activation.